Ligand effects as probes for mechanistic aspects of remote C–H bond activation by Iron(I) cations in the gas phase

Detlef Schröder, Helmut Schwarz *

Institut für Organische Chemie der Technischen Universität Berlin, Straße des 17. Juni 135, D-10623 Berlin, Germany

Abstract

The reactions of several ligated $Fe(L)^+$ cations with the model compound 4-heptanone have been examined by means of tandem and Fourier transform mass spectrometry. For the ligands L ($L = H_2O$, CO, CH_2O, C_2H_4, CH_3CHO, C_3H_6, C_2H_2, i-C_4H_8, CH_3CN, C_3H_6O, C_4H_6, and C_6H_6) under study, relative Fe^+ affinities have been evaluated by applying Cooks' kinetic method. In general, the ion–molecule reactions of the ligated $Fe(L)^+$ cations differ substantially from the behaviour of bare Fe^+ itself in that C–C bond activation as well as consecutive fragmentations are suppressed in favour of exclusive C–H bond activation for $Fe(L)^+$ cations. The product distributions obtained suggest classification of the ligands L into three categories. (i) The highly unsaturated ligands acetylene and 1,3-butadiene are actively involved in the reaction in that they induce transfer hydrogenation to yield ethene and butene, respectively, in addition, for $Fe(C_2H_2)^+$, ligand coupling via C–C bond formation is observed. (ii) The other ligands which act as spectator ligands display only moderate effects on the intrinsic reactivity of the 4-heptanone–Fe^+ system; further, it is observed that less energetic reaction products are formed with increasing binding energies of the ligands. (iii) Finally, the benzene ligand in $Fe(C_6H_6)^+$ prevents any bond activation of the incoming ketone and for which adduct formation is observed exclusively. The experimental findings lead to the conclusion that the activation barrier associated with the Fe^+-mediated dehydrogenation of (functionalized) alkanes amounts to ca. 12 kcal mol^{-1}.

Keywords: Iron; C–H bond activation; Mass spectrometry; Ligand effects; Bond energies; Transition-metal ions

1. Introduction

Attempts at selective functionalization of non-activated C–H bonds in organic molecules by transition metal complexes are of general interest as they encompass quite different areas of contemporary chemistry [1]. One of the most simple approaches to examine mechanisms and uncover fundamental principles of transition-metal-mediated C–H and C–C bond activation processes is provided by gas phase studies of reactions of "naked" or partially ligated metal ions by mass spectrometry. Within the last two decades, this approach has led to a significant body of knowledge about the elementary steps of metal-mediated C–H bond activation, and also periodic trends in the reactivity of first-, second-, and third-row transition metal ions

with various organic substrates became apparent [2]. Among the many substrates considered so far, most of the mechanistic examinations address the C–H and C–C bond activation of linear alkanes [3] or their monofunctionalized derivatives, e.g. amines [4], alcohols [5], ketones [6], acids [7], and nitriles [8].

Extensive studies of metal-mediated C–H and C–C bond activation of deuterium- or ^{13}C-labelled but otherwise unsubstituted alkanes revealed that often several processes compete with each other and that the positional integrity of the isotopic substitution is partially or completely lost in the course of the reaction [2,3]. The experimentally observed lack of regioselectivity can be traced back to the following reasons. (i) The more or less uniform van der Waals sphere of the alkanes does not favour the coordination of a metal cation to a particular segment of the molecule [9]. (ii) There exist competing trajectories for the initial insertion of the metal into the C–H and C–C bonds of an alkane, e.g. activation of primary vs. secondary C–H bonds [3e,f].

(iii) Reversible β-hydrogen transfer processes within the reaction intermediates may result in an overall H–D equilibration [10]. In marked contrast, in monosubstituted alkanes the metal ion is first coordinated to the functional group which serves as a dative ligand. As a consequence, this linkage ("docking") of the transition-metal ion to a heteroatom functionality leads to a high regio- and even stereoselectivity in metal-mediated C–H bond activation of the hydrocarbon backbone [2]. For example, a series of transition metal cations mediate selective C–H bond activation of terminal positions of aliphatic nitriles and carbonyl compounds [2,6–8]. In analogy to Breslow's terminology [11] these processes have been referred to as "remote functionalization" of substituted alkanes in the gas phase [12], and a visualization of a simplified mechanism for C–H and C–C bond cleavage of 4-heptanone by bare Fe^+ is depicted in Scheme 1.

The mechanism of remote functionalization in the gas phase was derived from detailed state-of-the-art mass spectrometric studies of extensively labelled substrates [12]. Within this context, the reactions of ketone–Fe^+ complexes are particularly telling in that competing side reactions hardly occur and so do not hamper the analysis of the processes of interest, and, moreover, C–H bond activation occurs with a high degree of regioselectivity. For the sake of better understanding of this article it is perhaps appropriate to recall the central aspects of previous findings with respect to the regioselectivity and the reaction mechanism operative in ketone–Fe^+ systems [6,7,13]. (i) For ketones with small side chains, e.g. acetone, α-C–C bond insertion of the metal and subsequent loss of an alkane is the dominant reaction pathway, e.g. $(CH_3)_2CO-Fe^+ \rightarrow FeCO^+ + C_2H_6$ [14]. (ii) Beginning with an n-propyl side chain remote functionalization becomes operative, and selective dehydrogenation as well as alkene losses from the $\omega/(\omega-1)$ positions occur [6b,13,15]. On further increase in the length of the alkyl chain(s) the regioselectivity decreases, since various positions remote from the functional group now become accessible for metal-mediated C–H and C–C bond activation [2]. (iii) The intramolecular H–D kinetic isotope effects (KIEs) k_{H_2}/k_{HD} associated with dehydrogenation of

carbonyl compounds by Fe^+ cations via remote functionalization range from 2.1 to 3.0 [13,16]. (iv) The rate-determining step associated with dehydrogenation of 1-Fe^+ (Scheme 1) corresponds to the reductive elimination of dihydrogen from the dihydrido insertion intermediate ($3 \rightarrow 4$-Fe^+); thus, C–H bond insertion of Fe^+ (1-$Fe^+ \rightarrow 2$) and β-hydrogen transfer ($2 \rightarrow 3$) are reversible within the time-scale of the experiment. Furthermore, the reversibility of the initial C–H bond activation in 4-heptanone–Fe^+ has been shown directly by performing an appropriate double-labelling experiment [6b]. (v) Despite the flexibility of alkyl side chains the dehydrogenation at the $\omega/(\omega-1)$ positions occurs diastereoselectively, involving a chiral Fe centre in the intermediate [7,16]. (vi) The remote functionalization of ketones is sensitive to geometric constraints; for example, the $\omega/(\omega-1)$ dehydrogenation of α-methylated 4-heptanone–Fe^+ complexes is affected by a large Ingold–Thorpe effect [17], while anellation of the alkyl chain with a cyclopropane ring prevents direct remote functionalization via initial C–H bond activation [18].

In this article, we propose inter alia a scheme to estimate the height of the activation barrier for Fe^+-mediated dehydrogenation of ketones via remote functionalization. The basic idea is to alter the internal energy of ketone–Fe^+ complexes by appropriate ligand exchange reactions of $Fe(L)^+$ complexes with the ketone of interest. As has been demonstrated previously, ligated $Fe(L)^+$ complexes can greatly enhance the selectivity for metal-mediated C–H bond activation in ion–molecule reactions at the expense of other competing processes [19]. In the present study as a representative substrate we have chosen 4-heptanone 1 (Chart 1) for the following reasons [6b,13]: (i) Fe^+ cations complexed to a keto group mediate regioselective functionalization of propyl sidechains at the $\omega/(\omega-1)$ positions. (ii) The symmetry of 4-heptanone allows a direct evaluation of the primary H–D KIE associated with C–H vs. C–D bond activation. (iii) As indicated in previous experiments and as will be demonstrated further below, for ketones with longer side chains the activation barrier associated with remote functionalization is even smaller as compared with 4-heptanone–Fe^+; therefore, the trapping and detection procedures used
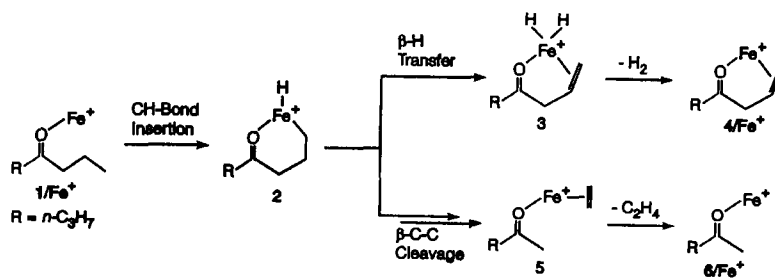
Scheme 1.
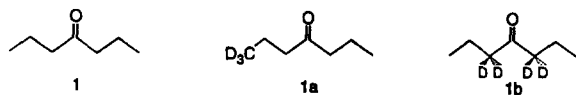
Form 1.

for 1–Fe$^+$ cannot be applied in the same manner for larger substrates. (iv) Finally, the volatilities of larger substrates which still fulfill the requirement of symmetrical alkyl chains, e.g. 4-nonanone or 5-undecanone [6b], are substantially lower as compared with 1, and therefore reactions of background contaminants in the vacuum system as well as minor impurities in the precursors may affect the accuracy of the experiments.

With respect to the use of deuterium-labelled substrates, a distinct difference of the present approach as compared with previous work should be pointed out. In most of the studies referred to in the preceding paragraphs, the magnitude of the H–D KIE associated with dehydrogenation served as a direct probe to derive information on regio- and stereoselectivity, reaction mechanisms, and/or rate-determining steps. In contrast to these mechanistic studies, here the KIEs are used simply to monitor the energetics of C–H bond activation as well as the existence of competing reaction pathways. Finally, the experimental findings together with thermochemical data as well as considerations of the energetics of ion–molecule reactions in general [20] permit the bracketting of the activation barrier associated with dehydrogenation of 4-heptanone by bare Fe$^+$ cations in the gas phase [21].

2. Experimental methods and thermochemical estimates

Most of the experiments were performed with a Spectrospin CMS 47X Fourier transform ion cyclotron resonance (FTICR) mass spectrometer, which has been described in detail elsewhere [22]. In brief, Fe$^+$ cations were formed by laser desorption/laser ionization [23] of an iron target in the external ion source of the instrument. By a system of electric potentials and lenses the resulting ions were transferred to the analyser cell which is located within a superconducting magnet (maximum field strength, 7.05 T). Subsequently, ^{56}Fe$^+$ was mass-selected using the FERETS technique [24], a computer-controlled ion ejection protocol which combines single-frequency ion ejection pulses with frequency sweeps to optimize ion isolation. Owing to the injection of the ions from the external ion source into the FTICR cell, the mass-selected ions exhibit an excess of kinetic energy as compared with thermal motion. In order to afford thermalization of Fe$^+$, argon was pulsed in several times (to a pressure and for a time which gives an estimate of 200 collisions), pumped out, and the Fe$^+$

ions were again mass selected; similar procedures were applied to Fe(L)$^+$ ions [25].

Ligated Fe(L)$^+$ cations were generated by ion–molecule reactions of mass-selected Fe$^+$ ions with appropriate substrates, i.e. Fe(CH$_2$O)$^+$ was obtained from Fe$^+$ and dimethylether [2], Fe(CO)$^+$ and Fe(C$_3$H$_6$O)$^+$ by reacting Fe$^+$ with acetone [14], Fe(H$_2$O)$^+$ from ligand exchange of Fe(C$_2$H$_6$)$^+$ and Fe(CO)$^+$ (both ions obtained from Fe$^+$ and acetone) in the presence of water [26]. The alkene complexes Fe(C$_2$H$_4$)$^+$, Fe(C$_3$H$_6$)$^+$, and Fe(i-C$_4$H$_8$)$^+$ were generated by reacting Fe$^+$ with propane and i-butane respectively [27]. The complexes Fe(C$_2$H$_2$)$^+$, Fe-(CH$_3$CHO)$^+$, Fe(CH$_3$CN)$^+$, Fe(C$_4$H$_6$)$^+$, and Fe(C$_6$H$_6$)$^+$ were obtained by consecutive ligand exchange reactions of Fe(C$_2$H$_4$)$^+$ with the corresponding neutrals [16a,19]; for the sake of simplicity, throughout this article acetone, butadiene, and benzene are referred to as C$_3$H$_6$O, C$_4$H$_6$, and C$_6$H$_6$. Except for water, the reagent gases for Fe(L)$^+$ generation were introduced to the FTICR cell via pulsed valves, such that these reactants hardly interfered with further experiments; owing to its relatively low volatility and its adsorption on the stainless steel walls of the instrument, water cannot be pumped away in the time available for the pulsed-valve operation sequence and, therefore, had to be leaked in continuously. For the subsequent ion–molecule reactions the Fe(L)$^+$ complexes were mass selected, thermalized by pulsed-in argon, again mass selected, and reacted with [1,1,1-D_3]-4-heptanone (1a) which was leaked in at typical pressures of ca. 5×10^{-9} mbar. Branching ratios were derived from the analysis of the pseudo-first-order reaction kinetics and are reported with a relative error of $\pm 10\%$. In order to avoid interferences with residual background reactants, double-resonance techniques have been applied; for example, in the measurement of Fe(CO)$^+$, the Fe(C$_3$H$_6$O)$^+$ ions formed by ligand exchange of Fe(CO)$^+$ with residual acetone were continuously ejected from the FTICR cell. It should be mentioned that the evaluation of precise intensities in FTICR mass spectrometry is associated with some systematic pitfalls [28]. In order to minimize these effects all spectra were recorded using identical mass windows for ion excitation and ion detection using 64K data size for the transient which was zero filled to 128 K prior to Fourier transformation. Despite the systematic errors which may be associated with intensity measurements, the technique described here leads to reproducible experimental results; furthermore, the measured KIEs associated with dehydrogenation of 1a by Fe(L)$^+$ complexes agree quite well with the data obtained from unimolecular dissociation of metastable ion complexes [13]. When necessary, exact ion masses were determined by high resolution experiments ($m/\Delta m >$ 100000) in order to ensure the assigned elemental composition of the product ions. All data were accumu-

lated and on-line processed using an ASPECT 3000 minicomputer.

Additional experiments were performed with a modified VG ZAB/HF/AMD 604 four-sector mass spectrometer of BEBE configuration (B stands for magnetic and E for electric sectors), which has been described elsewhere [29]. Ligated ketone–Fe$^+$ complexes were generated as described previously by chemical ionization of mixtures of ketone, ligand, and Fe(CO)$_5$ in a ca. 1:5:1 ratio [6b]. The ions of interest were accelerated to 8 keV kinetic energy and mass selected using B(1)E(1) at a resolution $m/\Delta m \approx 3000$. The unimolecular dissociations of metastable ions in the field-free region preceding the second magnet were recorded by scanning B(2) from the parent-ion mass to $m/z = 10$ within 30 s. All spectra were accumulated and on-line processed with the AMD–Intectra data system; 5 to 15 scans were averaged to improve the signal-to-noise ratio.

Chemicals were either commercially available or prepared according to well-known laboratory procedures and purified by distillation and preparative gas chromatography [15]. [D$_4$]-Ethene (Cambridge Isotope), [D$_6$]-acetone (Janssen Chimica), and [D$_6$]-benzene (Aldrich) were used as supplied. Gaseous formaldehyde was generated in an on-line apparatus [16a] by heating thoroughly dried para-formaldehyde in a glass tube which is directly connected to the chemical ionization source of the tandem mass spectrometer by a gas chromatography capillary (50 μm width, 25 cm length); the partial pressure of formaldehyde was adjusted by variation of the tube temperature. Because of the condensation of significant amounts of para-formaldehyde in the inlet lines, the apparatus had to be dismounted and cleaned after each use.
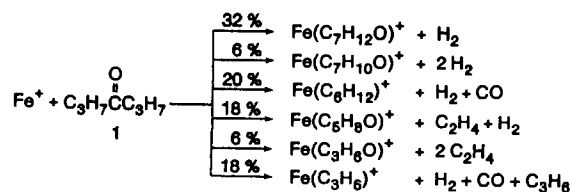
As far as reliable and consistent thermochemical data and ligand bond dissociation energies (BDEs) for the species of interest were available, these were taken from literature sources [30]. However, for a comparison of the reactivity of different Fe(L)$^+$ complexes, often more accurate relative BDEs of Fe(L)$^+$ complexes were needed. Unfortunately, the attempt to determine relative BDEs from the equilibrium constant of ligand exchange reactions of the type Fe(L)$^+$ + L' $\rightleftharpoons$ Fe(L')$^+$ + L by using FTICR mass spectrometry failed owing to the interfering formation of adduct-complexes Fe(L)$_n$(L')$_m^+$ (n, m = 0, 1, 2; $n + m = 2$) or to side reactions such as ligand coupling. As a consequence, equilibria between the monoligated Fe$^+$ complexes could not be established [31]. Therefore, we applied Cooks' kinetic method [32] for the evaluation of relative binding energies of various ligands to Fe$^+$. Following this approach, the ratio of L and L' losses from metastable Fe(L)(L')$^+$ complexes is related to the equilibrium constant K, which can be converted to $\Delta \Delta G$ of the ligand exchange reaction, or ΔBDE values for the two ligands [33]. For

this purpose mixed bis-ligand complexes of the type Fe(L)(L')$^+$ were generated by chemical ionization of mixtures of Fe(CO)$_5$ with the ligands L and L' present in ratios which gave maximal ion currents for the ion of interest. In order to account for the effect of mass discrimination in the ion detection, the intensities were weighted according to the mass differences when mass differences of fragment ions were large, e.g. loss of acetylene ($\Delta m = 26$) vs. acetone ($\Delta m = 58$) from Fe(C$_2$H$_2$)(C$_3$H$_6$O)$^+$ ($m/z = 140$) [34]. In order to monitor the occurrence of possible reactions between the ligands (H–D exchange or ligand coupling), in several cases one of the ligands was examined in its fully deuterated form, e.g. Fe(C$_2$D$_4$)(CH$_3$CHO)$^+$. However, it should be noted that Cooks' kinetic method is an approximate procedure and is subject to some shortcomings [32c], as for example the use of a temperature (we simply assumed the ion source temperature, i.e. 473 K) to describe the internal energy distribution. Therefore, these data should complement binding energies obtained by other methods; nevertheless, the ordering of the binding energies is reproduced correctly by this approach.

3. Results and discussion

The ion–molecule reaction of bare Fe$^+$ with 4-heptanone leads to a variety of products (Scheme 2) which can be explained in terms of remote functionalization of the alkyl side chains by the iron cation in terms of Scheme 1 and subsequent fragmentations of these products [19a]. For the sake of simplicity, if not stated otherwise we will always refer to **1** in the discussion, even when **1a** or **1b** was examined experimentally. As has been demonstrated previously [6b,15], the initial reactions of **1**–Fe$^+$ involve C–H and C–C bond activation of the terminal positions, and the variety of products can be ascribed to consecutive fragmentations of the primary products. These processes as well as the mechanistic aspects will not be pursued in the present discussion [19a]; we should only like to point out that careful analysis of the total product distribution leads to a 76:24 ratio of initial dehydrogenation vs. alkene losses.

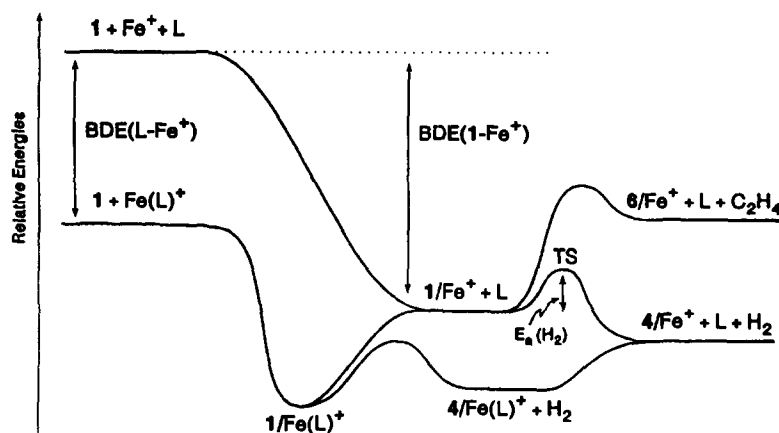Obviously, the consecutive fragmentations of the primary products originate from the large excess internal

$$
\begin{array}{l}
\text{O} \\
\| \\
\text{Fe}^+ + \text{C}_3\text{H}_7\text{CC}_3\text{H}_7 \\
\mathbf{1}
\end{array}
\begin{array}{l}
\xrightarrow{\textbf{32\%}} \text{Fe(C}_7\text{H}_{12}\text{O})^+ \ + \ \text{H}_2 \\
\xrightarrow{\textbf{6\%}} \text{Fe(C}_7\text{H}_{10}\text{O})^+ \ + \ 2\,\text{H}_2 \\
\xrightarrow{\textbf{20\%}} \text{Fe(C}_6\text{H}_{12})^+ \ + \ \text{H}_2 + \text{CO} \\
\xrightarrow{\textbf{18\%}} \text{Fe(C}_6\text{H}_8\text{O})^+ \ + \ \text{C}_2\text{H}_4 + \text{H}_2 \\
\xrightarrow{\textbf{6\%}} \text{Fe(C}_3\text{H}_6\text{O})^+ \ + \ 2\,\text{C}_2\text{H}_4 \\
\xrightarrow{\textbf{18\%}} \text{Fe(C}_3\text{H}_6)^+ \ + \ \text{H}_2 + \text{CO} + \text{C}_3\text{H}_6
\end{array}
$$

Scheme 2.

Fig. 1. Schematic potential energy hypersurface for the remote functionalization of 4-heptanone (1) by bare Fe^+ and $Fe(L)^+$ complexes. The qualitative energetics are derived from simple thermochemical estimates (for details, see Refs. [6b], [16a] and [19a]).

energy of the rovibrationally excited encounter complex $1-Fe^+$, when formed by coordination of the bare metal ion to the ketone. As will become obvious further below, to a first approximation the energy gain on complexation amounts to ca. 2 eV. In contrast, when unimolecular fragmentations of metastable $1-Fe^+$ ions are probed, the selectivity is larger as seen by (i) the absence of consecutive fragmentations and (ii) the slight

rise in ratio of dehydrogenation to alkene loss to 80 : 20 [6b,13,15]. This is simply due to the fact that the metastable ions stemming from a chemical ionization process at ca. 10^{-3} mbar and surviving for ca. 1 μs contain less excess internal energy as compared with the excited encounter complex $1-Fe^+$ which is formed in the absence of any stabilizing collisions under FTICR conditions at ca. 10^{-8} mbar.

Table 1
Ratio of the relative abundances for the unimolecular losses of the ligands L and L' from $Fe(L)(L')^+$ complexes and differences of the bond dissociation energies ΔBDE (kcal mol^{-1}) according to Cooks' kinetic method [a]

$Fe(L)(L')^+$	$Fe(L)^+ : Fe(L')^+$ [b]	ΔBDE [c,d]	Side reactions [e]
$Fe(H_2O)(CO)^+$	1.4	0.3	
$Fe(H_2O)(C_2D_4)^+$	52	3.7	
$Fe(CO)(CH_2O)^+$	11	2.3	
$Fe(CO)(C_2D_4)^+$	35	3.3	
$Fe(CO)(CH_3CHO)^+$	160	4.8	
$Fe(CO)(C_3H_6)^+$	310	5.4	
$Fe(CH_2O)(C_2H_4)^+$	3.2	1.1	
$Fe(C_2D_4)(CH_3CHO)^+$	2.6	0.9	
$Fe(C_2D_4)(C_3H_6)^+$	16	2.6	H–D equilibration
$Fe(C_2H_4)(C_2H_2)^+$	40	3.5	$C_4H_6(5\%)$
$Fe(C_2D_4)(i-C_4H_8)^+$	110	4.4	H–D equilibration
$Fe(CH_3CHO)(C_3H_6)^+$	3.9	1.3	
$Fe(CH_3CHO)(i-C_4H_8)^+$	37	3.4	
$Fe(CH_3CHO)(C_3D_6O)^+$	420	5.7	$CH_4(10\%)$
$Fe(C_3H_6)(C_2H_2)^+$	1.9	0.6	$H_2(20\%), C_2H_4(40\%)$
$Fe(C_3H_6)(i-C_4H_8)^+$	13	2.4	$H_2(15\%), C_2H_4(35\%)$
$Fe(C_2H_2)(CH_3CN)^+$	29	3.2	
$Fe(i-C_4H_8)(CH_3CN)^+$	10	2.2	
$Fe(i-C_4H_8)(C_3D_6O)^+$	12	2.3	
$Fe(CH_3CN)(C_3D_6O)^+$	1.1	0.1	HCN(2%)
$Fe(CH_3CN)(C_4H_6)^+$	10	2.2	
$Fe(C_3D_6O)(C_4H_6)^+$	6.5	1.8	$CD_3CHO(5\%)$
$Fe(C_4H_6)(C_6H_6)^+$	240	5.2	

[a] ΔBDE are calculated assuming a temperature of 473 K; see text. [b] The experimental uncertainty in L : L' is dependent on the magnitude and the intensity of unimolecular decay of $Fe(L)(L')^+$, roughly, the errors range from 5% for L : L' = 1 to 20% for L : L' = 500. [c] $\Delta BDE = BDE(L'-Fe^+)$ − $BDE(L-Fe^+)$, thus, L' is the more strongly bound ligand. [d] Because of the logarithmic relationship between the abundances for L : L' losses and ΔBDE the errors are dependent on the absolute values and range from ±0.1 to ±1 kcal mol^{-1}. [e] Here, H–D exchange between the ligands or side reactions are mentioned; intensities (in parentheses) are given as percentages of the intensity for the loss of L. Note that these processes have been neglected in the calculation of relative BDEs.

One way to moderate the reactivity of a bare metal cation is to complex the metal with ligands L. As far as the ion–molecule reactions of $Fe(L)^+$ complexes with **1** are concerned, the presence of an additional ligand L might cause the following effects. (i) Ligand exchange of L for **1** leads to $1-Fe^+$; assuming that the $Fe(L)^+$ ions are sufficiently thermalized, this process will take place provided that $BDE(1-Fe^+)$ is close to or exceeds $BDE(L-Fe^+)$. The internal energy of $1-Fe^+$ formed in this manner can be related to the difference of the BDEs and may lead either to a radiative stabilization [35] of $1-Fe^+$ such that no further C–H or C–C bond activation is possible, or to the dissociation of $1-Fe^+$ via remote functionalization which will generally be confined to the lowest energy demanding process, i.e. the dehydrogenation channel $(1-Fe^+ \rightarrow 4-Fe^+)$. Alternatively, remote functionalization may occur within the ligated complex giving rise to $4-Fe(L)^+$ and $6-Fe(L)^+$. (ii) C–H and C–C bond activation may be suppressed by the additional ligand, such that the only product is the $1-Fe(L)^+$ adduct complex which is stabilized via radiative or collisional cooling processes [19,31,35]. (iii) Within the encounter complex the ligand L may open up new chemical pathways, such that the reactivity of the ligated complex, $1-Fe(L)^+$, differs fundamentally from that of $1-Fe^+$ itself [36]. An entirely qualitative potential energy surface for the reactions of $Fe(L)^+$ with **1** is depicted in Fig. 1; note that the channels leading to $1-Fe^+$, $4-Fe^+$, and the adduct complexes may well compete with each other.

3.1. Evaluation of the bond dissociation energies of $Fe(L)^+$ complexes

As already mentioned, one crucial parameter which will determine the products of the ion–molecule reac-

tion of $Fe(L)^+$ with **1** is $BDE(L-Fe^+)$. Although for some of the ligands under study quite accurate absolute BDEs are reported in the literature, the approach applied here for the estimation of the activation barrier associated with dehydrogenation of $1-Fe^+$ (see below) requires even more precise information on the relative BDEs of the various ligands. Therefore, before considering the ion–molecule reactions of $Fe(L)^+$ complexes with **1**, we address the relative Fe^+ affinities of the ligands from which approximate absolute BDEs can be evaluated by anchoring this scale to an absolute value.

The relative BDEs (Table 1) were determined from the intensities of the fragment ions resulting from unimolecular ligand losses of L and L′ from mixed bisligand complexes of the type $Fe(L)(L')^+$ according to Cooks' kinetic method [32]. The $\Delta BDEs$ derived by this approach are internally consistent. For example, for $Fe(CO)^+$ and $Fe(C_2H_4)^+$ a ΔBDE of 3.3 ± 0.2 kcal mol^{-1} is derived from the couple $Fe(CO)(C_2H_4)^+$; this number is in good agreement with the value of 3.4 ± 0.4 kcal mol^{-1} as obtained by combining the data of $Fe(CH_2O)(C_2H_4)^+$ and $Fe(CO)(CH_2O)^+$. As far as the internal energy of the ions is concerned, the effective temperatures of collisionally activated proton-bound dimers have been derived from comparison of measured $\Delta BDEs$ with well-known literature values for the corresponding proton affinities [32c,d]. However, this approach is not applicable in our system owing to the lack of a reliable, large enough set of absolute BDEs; for example, the most recent and accurate absolute BDEs for $Fe(C_2H_4)^+$ and $Fe(C_3H_6)^+$ [30d] are identical within experimental error which not only is counterintuitive but also contradicts the present findings for $Fe(C_2H_4)(C_3H_6)^+$. For the time being, we are left to rely on the simple assumption that the internal energy distribution of the metastable ions generated by chemi-

Table 2
Approximate ligand bond dissociation energies $BDE(L-Fe^+)$ (kcal mol^{-1}) as calculated from the relative values given in Table 1 and literature values for comparison. For the evaluation of the data, $BDE(C_2H_4-Fe^+) = 34.5$ kcal mol^{-1} [30d] was used as anchor point [a]

| $Fe(L)^+$	This work [b]	Literature
$Fe(H_2O)^+$	30.8 ± 0.2	30.6 ± 1.1 [30d]
$Fe(CO)^+$	31.2 ± 0.2	31.3 ± 1.8 [30d]
$Fe(CH_2O)^+$	33.4 ± 0.2	
$Fe(C_2H_4)^+$	34.5 [30d]	34 ± 2 [37]; 34.5 ± 1.4 [30d]
$Fe(CH_3CHO)^+$	35.7 ± 0.3	
$Fe(C_3H_6)^+$	37.0 ± 0.3	37 ± 2 [37]; 34.3 ± 1.6 [30d]
$Fe(C_2H_2)^+$	38.0 ± 0.5	32 ± 6 [38], ≈ 37 [39]
$Fe(i-C_4H_8)^+$	39.1 ± 0.5	
$Fe(CH_3CN)^+$	41.3 ± 0.7	
$Fe(C_3D_6O)^+$	41.4 ± 0.7	
$Fe(C_4H_6)^+$	43.4 ± 1.0	48 ± 5 [2a]
$Fe(C_6H_6)^+$	48.6 ± 2.0	55 ± 5 [2a] [d]

[a] Differences between deuterated and non-deuterated ligands and entropy effects were neglected. [b] Experimental errors range from ± 0.3 to ± 2 kcal mol^{-1}, depending on the errors of ΔBDE as determined by applying Cooks' kinetic method (Table 1), however, the absolute error may be larger and it relies completely on the accuracy of the anchor point as well as on the definition of temperature. [d] For a theoretical study, see Ref. [40].

cal ionization corresponds to the ion source temperature (473 K).

In order to convert the ΔBDEs to absolute BDEs, it is necessary to relate the Fe^+ affinity scheme to a reference; for this purpose, $BDE(C_2H_4-Fe^+) = 34.5$ kcal mol^{-1} from Ref. [30d] was taken as an anchor point. As demonstrated by the data shown in Table 2, the BDEs obtained using this approach compare well with previous experimental findings. Moreover, for $Fe(CO)^+$ and $Fe(C_2H_4)^+$ the assumption of an effective ion temperature of 473 K leads to ΔBDE = 3.3 kcal mol^{-1} which agrees well with the difference of 3.2 kcal mol^{-1} for the absolute BDEs of $Fe(CO)^+$ and $Fe(C_2H_4)^+$ as reported by Armentrout and Kickel [30d]. In principal, Cooks' kinetic method only permits measurements of ΔBDE ≤ 5 kcal mol^{-1}, since for larger ΔBDE the experimental errors associated with intensity measurements as well as interferences with background gases in the mass spectrometer become too large. Therefore, in order to cover a wider range of BDEs the data have to be evaluated in a stepwise manner with the consequence that the experimental errors accumulate with the distance from the anchor point. Furthermore, with increasing BDEs of the ligands and also with increasing ligand sizes the internal energy content of the metastable $Fe(L)(L')^+$ complexes may rise to higher effective temperatures which will directly affect the estimated ΔBDE. As a case in point, we would like to refer to the enormous kinetic shifts in the unimolecular dissociation of fullerene cations [41]. Therefore, the quoted accuracy of ± 2.0 kcal mol^{-1} for $BDE(C_6H_6-Fe^+)$ does not include systematic errors which may arise from the definition of ion temperature, entropy effects, the occurrence of competing processes such as ligand coupling with subsequent fragmentation of the new complexes (e.g. C_2H_4 loss from $Fe(C_3H_6)(i-C_4H_8)^+$), as well as the anchor point chosen. In addition, this value relies on a single (and extreme) ratio of 240 for $Fe(C_6H_6)(C_4H_6)^+$. Because of these sources of systematic errors, the disagreement between BDE $(C_6H_6-Fe^+) = 48.6 \pm 2.0$ kcal mol^{-1} as derived in this work and the literature value of 55 ± 5 kcal mol^{-1} [2a] should not imply that only one of the two values is correct; rather, it emphasizes the need for more precise absolute metal ligand binding energies in order to assess the reliability of the different experimental approaches. In fact, the BDE of $Fe(C_6H_6)^+$ derived in this study is in reasonable agreement with a very recent determination of $BDE(C_6H_6-Fe^+) = 51.4 \pm 2$ kcal mol^{-1} by Armentrout and coworkers [42].

3.2. Ion–molecule reactions of $Fe(L)^+$ with $C_3H_7COC_3H_7$ (1)

Basically, under FTICR conditions the products of the ion–molecule reactions of $Fe(L)^+$ with 1 can be
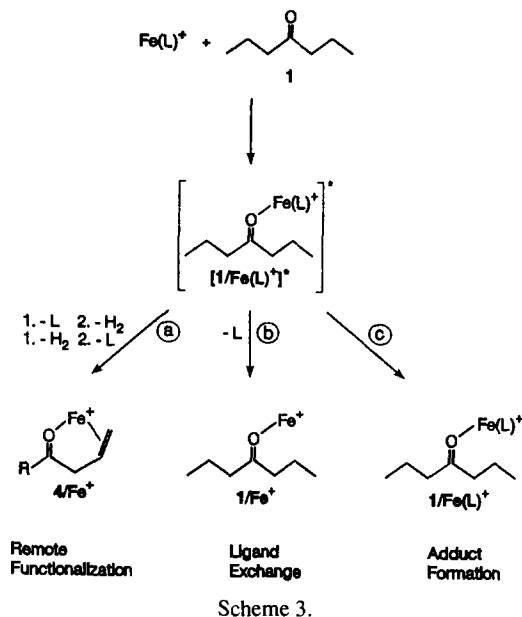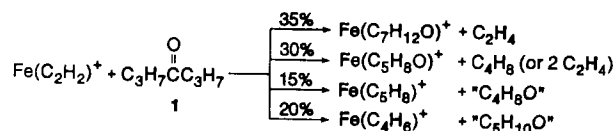

Scheme 3.

classified in terms of three principal reaction products (Scheme 3). (i) Two reaction pathways (path a) may lead to the formation of the dehydrogenation product $4-Fe^+$. Either ligand exchange of L for 1 to yield excited $1-Fe^+$ is followed by rapid dehydrogenation via remote functionalization, or dehydrogenation occurs within the excited encounter complex $1-Fe(L)^+$ and, subsequently, the ligand L is lost. (ii) Ligand exchange of L for 1 may lead to stable $1-Fe^+$ (path b). (iii) The excited adduct complex $1-Fe(L)^{+*}$ might undergo either radiative stabilization to yield stable $1-Fe(L)^+$ or remote functionalization leading to dehydrogenation and/or alkene losses, but not that of the ligand L, such that $4-Fe(L)^+$ and $6-Fe(L)^+$ are formed as reaction products. For the sake of clarity, the intensities of these products will be summed and assigned as adduct formation (path c). Experimentally, except for bare Fe^+ itself (see above) and the acetylene complex $Fe(C_2H_2)^+$ (see below) no further reaction products than $1-Fe^+$, $4-Fe^+$, $1-Fe(L)^+$, $4-Fe(L)^+$ and $6-Fe(L)^+$ are observed.

For all $Fe(L)^+$ complexes under study, the additional ligand L does not alter the regioselectivity of the Fe^+-mediated bond activations of 1, since dehydrogenation to yield $4-Fe^+$ or $4-Fe(L)^+$ as well as alkene losses to yield $6-Fe^+$ or $6-Fe(L)^+$ involve the terminal positions exclusively, i.e. 1a leads only to H_2-HD and $C_2H_4-C_2H_2D_2$ losses respectively, whereas no products of C–D bond activation are observed for 1b. Thus, the reaction products can be described in terms of the remote functionalization mechanism depicted in Scheme 1 for Fe^+ as well as for $Fe(L)^+$. Not surprisingly, in the reaction of $Fe(L)^+$ with 1 C–C bond activation leading to unligated $6-Fe^+$ is completely suppressed, reflecting the substantially higher energy demand of C–C bond activation as compared with C–H bond activation en

route to dehydrogenation [6b,19]. While this energy is available in the ion–molecule reaction of the bare metal ion, part of it is consumed by the energy required to evaporate the ligand L from the encounter complex $1-Fe(L)^{+*}$ when $Fe(L)^+$ complexes react (Fig. 1). Moreover, the data in Table 3 display a clear dependence of the product distribution on the relative BDEs of the $Fe(L)^+$ complexes: with increasing BDEs the relative abundances of the ligand exchange channel as well as of the adduct complexes increase at the expense of the dehydrogenation pathway to yield $4-Fe^+$. Likewise, the magnitudes of the KIEs k_{H_2}/k_{HD} associated with formation of $4-Fe^+$ rise from 1.9 for bare Fe^+ to 2.9 for acetone–Fe^+, which agrees well with the conclusion that the internal energy content of rovibrationally excited $1-Fe^+$ decreases with increasing BDEs of the ligands L in the $Fe(L)^+$ complexes which served as precursors in the ligand exchange reaction. Furthermore, the KIE $k_{H_2}/k_{HD} = 2.7$ associated with the unimolecular dissociation of metastable $1-Fe^+$ [6b,13] supports the assumption that the internal energy content of ionic transition metal complexes sampled in metastable ion spectra in the microsecond timeframe is significantly lower than BDE $(1-Fe^+)$.

However, the product distribution for two of the $Fe(L)^+$ complexes clearly deviates from this trend, namely the complexes of the highly unsaturated hydrocarbon ligands $Fe(C_2H_2)^+$ and $Fe(C_4H_6)^+$. For the butadiene complex, $Fe(C_4H_6)^+$, the dehydrogenation product $4-Fe^+$ is formed exclusively, and the kinetic isotope effect associated with its formation is rather low, i.e. $k_{H_2}/k_{HD} = 1.6$. For the acetylene complex

Scheme 4.

$Fe(C_2H_2)^+$ the situation becomes even more complex in that C–C bond activation also takes place (Scheme 4). Consequently, these ligands do not serve as mere "spectator" ligands which just mediate the reactivity of the metal ion; rather, they participate actively in promoting new reactions. For example, the butadiene ligand in $Fe(C_4H_6)^+$ serves as an acceptor for the hydrogen being released via Fe^+-mediated remote functionalization of the ketone [19a,43]; this process has also been referred to as transfer hydrogenation [44]. Thus, while C–H bond activation of the terminal positions still takes place [45], the energetics are changed drastically, since the butadiene is hydrogenated to butene in the course of the reaction, and the heat of hydrogenation $(-29.5$ kcal mol^{-1}) is dissipated as internal energy over the whole system. As a consequence the KIE k_{H_2}/k_{HD} associated with the formation of $4-Fe^+$ decreases to 1.6. For the acetylene ligand, the products of the reaction of $Fe(C_2H_2)^+$ with 1 demonstrate that not only transfer hydrogenation takes place $(C_2H_2 \rightarrow C_2H_4)$, but in addition new C–C bonds between acetylene and parts of the ketone moiety are formed as demonstrated by the appearance of the products $Fe(C_5H_8)^+$ and $Fe(C_4H_6)^+$. Similar ligand coupling processes with dienes and alkynes have been reported previously [46] and will

Table 3
Branching ratios of the three basic reaction channels for the ion–molecule reaction of ligated Fe^+ cations with $[1,1,1-D_3]$-4-heptanone; for notation, see Fig. 1 and Scheme 3 (data normalized to 100%)

	BDE(Fe$^+$–L) (kcal mol^{-1}) [a]	Adduct complexes [b] $1-Fe(L)^+$, $4-Fe(L)^+$, $6-Fe(L)^+$	Ligand exchange $1-Fe^+$	Combined losses of L + H$_2$ $4-Fe^+$	KIE associated with formation of $4-Fe^+$ [c]
Fe^+	—	— [d]	— [d]	76 [d,e]	1.9
$Fe(H_2O)^+$	30.8		2	98	2.7
$Fe(CO)^+$	31.2		1	99	2.5
$Fe(CH_2O)^+$	33.4		3	97	2.6
$Fe(C_2H_4)^+$	34.5	6	35	59	2.7
$Fe(CH_3CHO)^+$	35.7	15	35	50	2.8
$Fe(C_3H_6)^+$	37.0	12	36	52	2.8
$Fe(C_2H_2)^+$	38.0			35 [e]	2.8
$Fe(i-C_4H_8)^+$	39.1	27	30	43	2.9
$Fe(CH_3CN)^+$	41.3	16 + 66 [f]	7	11	2.8
$Fe(C_3H_6O)^+$	41.4	25 + 49 [g]	13	13	2.9
$Fe(C_4H_6)^+$	43.4			100	1.6
$Fe(C_6H_6)^+$	48.6	100			—

[a] See Table 2. [b] Unless mentioned otherwise, the given intensity refers to that of $1-Fe(L)^+$. [c] The experimentally measured ratio of $[(1a-Fe^+)-H_2]^+$ to $[(1a-Fe^+)-HD]^+$ has been corrected for the natural abundance of the ^{13}C isotopes; experimental uncertainty, ±0.1. [d] On principal grounds these processes are impossible for unligated Fe^+; the entry in the fifth column refers to dehydrogenation to yield $4-Fe^+$. [e] In addition, also C–C bond activation processes, consecutive fragmentations, and for $Fe(C_2H_2)^+$ also ligand coupling take place (Scheme 4). [f] This notation indicates that 16% adduct formation and 66% remote functionalization within the adduct complexes are observed (Scheme 5). [g] For notation, see footnote f.

therefore not be pursued further. The fact that acetylene and butadiene do not act as mere spectator ligands excludes these ligands from the comparison of the effect of BDE on the ion–molecule reactions of $Fe(L)^+$ complexes with 1.
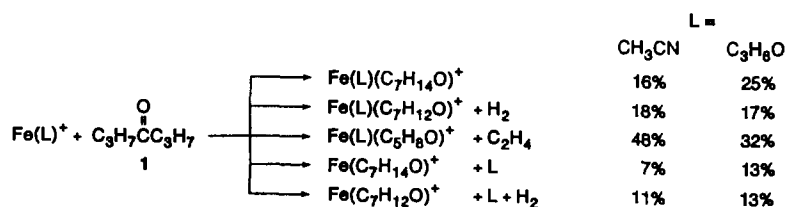
For $L = CH_3CN$ and C_3H_6O, also C–H and C–C bond activation of the ketone without accompanying loss of the ligands is observed in that dehydrogenation of the adduct complexes $(1-Fe(L)^+ \rightarrow 4-Fe(L)^+ + H_2)$ and alkene losses $(1-Fe(L)^+ \rightarrow 6-Fe(L)^+ + C_2H_4)$ from the terminal positions take place (Scheme 5). These bond cleavage processes involve the terminal positions of the ketone exclusively, since only H_2/HD and $C_2H_4/C_2H_2D_2$ are lost when 1a is allowed to react with these two $Fe(L)^+$ complexes and only H_2 and C_2H_4 are formed in the reaction of the $[\alpha,\alpha'-D_4]$ isotopologue 1b with $Fe(L)^+$ (L = acetonitrile, acetone). Although these processes can therefore still be described in terms of the remote functionalization concept (Scheme 1), the energetics as well as the rate-determining steps differ substantially from those of the unligated $1-Fe^+$ complexes. For example, in the reactions of $Fe(CH_3CN)^+$ and $Fe(C_3H_6O)^+$ with 1 the ratio between C–H and C–C bond activation is reversed to 27:73 and 35:65 respectively, as compared with 76:24 for the reaction of bare Fe^+ with 1 and 80:20 for the dissociation of metastable $1-Fe^+$. Furthermore, for $L = CH_3CN$ and C_3H_6O the kinetic isotope effects k_{H_2}/k_{HD} associated with dehydrogenation within the ligand complexes to yield $4/Fe(L)^+$ decrease to 2.0 and 2.3 respectively, while simultaneously those for the alkene losses increase to 2.2 and 2.3 respectively, as compared with the reaction of the bare Fe^+ [13b]. Indeed, the larger KIEs associated with alkene losses in the reaction of 1 with $Fe(L)^+$ indicate that the rate-determining steps of C–C bond activation differ substantially from those derived for the reaction of the unligated Fe^+. As far as the change in the branching ratio of H_2 vs. C_2H_4 losses is concerned we propose that the dehydrogenation channel is disfavoured on energetic grounds: for a series of transition metal complexes the first and the second metal–ligand binding energies $BDE(L_nM^+-L; n = 0, 1)$ are quite similar, and in several cases $BDE(LM^+-L)$ even exceeds $BDE(M^+-L)$, whereas on further increase of the coordination number the BDEs decrease significantly [30d,47]. Therefore, to a first

approximation $4-Fe^+$ will experience a larger stabilization by the C–C double bond formed in the dehydrogenation process as compared with ligated $4-Fe(L)^+$. As a consequence, dehydrogenation of $1-Fe(L)^+$ will be less exoergic than that of $1-Fe^+$ itself, whereas the reaction enthalpy of the C–C loss channel will hardly be affected. In addition to this thermodynamic reasoning, kinetic factors are likely also to play a role in the partitioning of the C–H and C–C bond activation channels; however, these effects cannot be assessed from the present set of data.

Despite these mechanistically intriguing changes, the occurrence of dehydrogenation as well as alkene losses in the reactions of $Fe(L)^+$ with 1 demonstrates that remote functionalization is not limited to the interaction of a bare metal cation with an organic substrate; even additional ligands do not prevent C–H and C–C bond activation from occurring via this mechanism. We note in passing that dehydrogenations of bisligated complexes of the type $1-Fe(L)_2^+$ (L = 1, 4) have been observed [16a], although these processes proceed significantly more slowly as compared with the reactions described here.

3.3. Activation barrier associated with dehydrogenation of $1-Fe^+$

In the condensed phase the height of an activation barrier E_a of a chemical reaction is usually derived from the temperature dependence of the reaction rate constant expressed in terms of the Arrhenius equation. In gas phase ion chemistry this approach is often not possible in principle [20]. For example, in an ion–molecule reaction in the dilute gas phase, attractive van der Waals' interactions will lead to a rovibrationally excited encounter complex of the reactants which contains quite a lot of excess energy in terms of temperature, even when the isolated reactants were thoroughly thermalized. Moreover, there exist this further fundamental difference: any ion–molecule reaction in the diluted gas phase represents a microscopic event with a certain energy demand, the critical energy, for a particular rearrangement process, whereas the Arrhenius formalism defines a macroscopic activation barrier. Therefore, the precise figure for the activation barrier of remote functionalization should not be overinterpreted; rather,

| | | L = | | |
		CH_3CN	C_3H_6O
	$Fe(L)(C_7H_{14}O)^+$	16%	25%
	$Fe(L)(C_7H_{12}O)^+ + H_2$	18%	17%
$Fe(L)^+ + C_3H_7\overset{O}{\overset{\shortparallel}{C}}C_3H_7$	$Fe(L)(C_5H_8O)^+ + C_2H_4$	48%	32%
1	$Fe(C_7H_{14}O)^+ + L$	7%	13%
	$Fe(C_7H_{12}O)^+ + L + H_2$	11%	13%

Scheme 5.

it serves as a qualitative guide for the understanding of C–H bond activation processes.

One approach to experimentally estimate gas phase activation barriers is based on variation in the internal energy content ε_i of the ion of interest. In FTICR mass spectrometry different internal energy contents can be achieved by generating rovibrationally excited $1-Fe^+$ via ligand exchange reactions of thermalized $Fe(L)^+$ ions with neutral 1, where ε_i is dependent on the BDEs of 1 and L to Fe^+, i.e. $\varepsilon_i \leq BDE(1-Fe^+) - BDE(L-Fe^+)$. Consequently, whenever the internal energy content of the $1-Fe^+$ formed in this way is lower than the energy demand for further reactions, the complex will be stable as such. However, when the internal energy content of $1-Fe^+$ exceeds the height of the activation barrier associated with the energetically lowest reaction pathway, consecutive products from (excited) $1-Fe^+$ can evolve. As has been discussed above and illustrated in Scheme 1, for $1-Fe^+$ the dehydrogenation pathway corresponds to the energetically lowest-lying exit channel. Thus, an estimate for the height of the activation barrier $E_a(H_2)$ associated with dehydrogenation of $1-Fe^+$ can be derived from the energy difference of $BDE(1-Fe^+)$ and $BDE(L-Fe^+)$ for that ligand L for which consecutive formation of $4-Fe^+$ via excited $1-Fe^+$ takes just place, i.e. $1 + Fe(L)^+ \rightarrow 1-Fe(L)^{+*} \rightarrow 1-Fe^+ + L \rightarrow 4-Fe^+ + H_2 + L$.

In practice, the situation is not that straightforward, since formation of $4-Fe^+$ can occur via two different routes, i.e. either with or without the ligand L (Fig. 1). Therefore, the occurrence of $4-Fe^+$ as such in an ion–molecule reaction of 1 with $Fe(L)^+$ is not indicative of the height of $E_a(H_2)$. As the most illustrative example we would like to refer to the reaction of $Fe(C_4H_6)^+$ in which, despite the high BDE of the butadiene ligand, $4-Fe^+$ is formed exclusively which is due to transfer hydrogenation and concomitant formation of butene. However, what is indicative of the

magnitude of $E_a(H_2)$ is the formation of stable $1-Fe^+$: in terms of gas phase ion chemistry [20], the formation of $1-Fe^+$ from $Fe(L)^+$ and 1 represents a ligand exchange reaction which should not be subject to significant activation barriers in excess of its thermochemical threshold, and it should be facile and rapid if it is energetically allowed. Therefore, whenever ΔBDE of the ligand L and 1 is smaller than $E_a(H_2)$, ligand exchange to yield stable $1-Fe^+$ should compete with formation of $4-Fe^+$ via remote functionalization within the mixed bisligated complex $1-Fe(L)^+$ (Fig. 1). In accordance with this, for the most weakly bonded ligands, $L = H_2O$, CO, and CH_2O, the intensity of $1-Fe^+$ is rather low, while it increases for the ligands with higher BDEs. Thus, the onset of the signal for $1-Fe^+$ determines that point on the energy scale at which the internal energy of rovibrationally excited $1-Fe^+$ is no longer sufficient to induce its metastable decomposition to $4-Fe^+$ prior to radiative or collisional cooling. The intensities of the three basic reaction channels are displayed in Fig. 2, and it is apparent that the onset for the formation of long-lived $1-Fe^+$ is at a $BDE(L-Fe^+)$ of ca. 34 kcal mol^{-1}. Thus, for ligands with a BDE of less than 34 kcal mol^{-1}, initial ligand exchange yields "hot" $1-Fe^+$, which subsequently undergoes rapid dehydrogenation to yield $4-Fe^+$. For the ligands with higher BDEs ligand exchange to yield long-lived $1-Fe^+$ does take place, and we conclude that remote functionalization occurs within the ligand complexes, i.e. ligand loss succeeds dehydrogenation. Experimentally, remote functionalization within the ligated complexes becomes apparent for $L = CH_3CN$ and C_3H_6O as the formation of $4-Fe(L)^+$ and $6-Fe(L)^+$, as described above. Finally, for the most strongly bonded benzene ligand, any further reactivity of $Fe(C_6H_6)^+$ with 1 is prevented and only adduct formation is experimentally observed.

The suggestion that remote functionalization of the ketone ligand in the adduct complex $1-Fe(L)^+$ does not

Table 4
Neutral losses in the unimolecular dissociation of $1-Fe(L)^+$ complexes (data normalized to 100%) [a]

L	H_2	C_2H_4	L	$L + H_2$	1	Other neutrals
CO			100			
C_2D_4 [b]	2		89	9		
CH_3CHO	10	5	78	5		CH_4 (2%)
CH_3CN	21	43	28	5	1	$CH_3^{\bullet}$ (2%)
C_3H_6O	25	35	31	5	1	$CH_3^{\bullet}$ (3%)
C_4H_6	1	3	5 [c]	90	1	
C_6H_6	1	1	13 [d]	6	79	

[a] The elemental composition of the neutrals was derived from comparative studies of 1, 1a, and 1b as well as the fully deuterated ligands C_3D_6O and C_6D_6. [b] C_2D_4 was used to distinguish ligand loss from ethene stemming from C–C bond activation of the ketone. [c] The precise ratio of $1-Fe^+$ to $Fe(C_4H_6)^+$ amounts to 100:11; thus, according to Cooks' kinetic method, $BDE(1-Fe^+) - BDE(C_4H_6) = 2.1 \pm 0.5$ kcal mol^{-1}, however, the intense side reactions may affect the analysis substantially. [d] According to Cooks' kinetic method $BDE(C_6H_6-Fe^+) - BDE(1-Fe^+) = 1.8 \pm 0.3$ kcal mol^{-1}; however, side reactions may also affect the analysis.
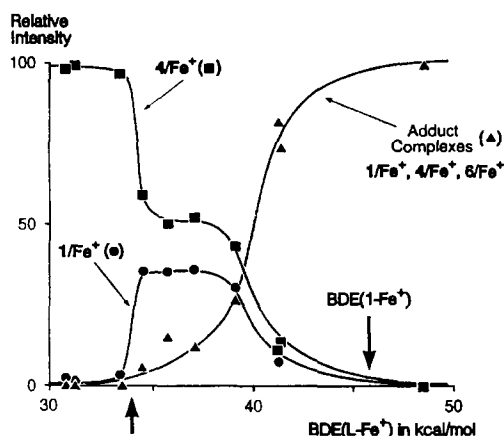
Fig. 2. Dependence of the product distribution of the ion–molecule reactions of Fe(L)$^+$ ions with 4-heptanone on BDE(L–Fe$^+$). For the sake of clarity, the intensities of the adduct complexes 1-Fe(L)$^+$, 4-Fe(L)$^+$, and 6-Fe(L)$^+$ are summed up. The arrows indicate the onset for the ligand exchange product 1-Fe$^+$ and BDE (1-Fe$^+$). The full lines serve only to guide the eyes and should not imply a certain algebraic function. For the notation of the reaction channels and explicit data, see text and Table 3.

occur for weakly bound ligands L is further supported by the unimolecular fragmentation patterns of independently generated mixed bisligated complexes 1-Fe(L)$^+$ (Table 4): whereas for L = CO, ligand loss is observed exclusively, for the ligands with higher BDEs losses of H$_2$ and C$_2$H$_4$ without loss of the ligand take place (i.e. 1-Fe(L)$^+$ → 4-Fe(L)$^+$ + H$_2$ and 1-Fe(L)$^+$ → 6-Fe(L)$^+$ + C$_2$H$_4$), and these processes gain in intensity proceeding from L = C$_2$D$_4$ to C$_3$H$_6$O. Similar to the FTICR experiment, in the unimolecular dissociation of the butadiene complex transfer hydrogenation takes place, such that the combined loss of C$_4$H$_6$–H$_2$ dominates. The benzene complex 1-Fe(C$_6$H$_6$)$^+$ is almost unreactive in that simple ligand losses dominate. Finally, we can once again apply Cooks' kinetic method for the evaluation of the unknown BDE(1-Fe$^+$): from the relative abundances of the unimolecular losses of the hydrocarbon ligands and those of 1 from 1-Fe(C$_4$H$_6$)$^+$ and 1-Fe(C$_6$H$_6$)$^+$, an estimate of BDE(1-Fe$^+$) ≈ 46 kcal mol^{-1} is obtained.

Let us summarize the experimental findings and the values used in constructing Fig. 1. (i) When excited 1-Fe$^+$ is formed in a ligand exchange reaction of 1 with Fe(L)$^+$ complexes with BDE(L–Fe$^+$) < 34 kcal mol^{-1}, the species is too hot to survive long enough prior to ion detection on the millisecond timescale of FTICR mass spectrometry. (ii) For ligands with larger BDEs, formation of stable 1-Fe$^+$ and remote functionalization within the adduct complexes 1-Fe(L)$^+$ compete with each other. (iii) According to Cooks' kinetic method BDE(1-Fe$^+$) amounts to ca. 46 kcal mol^{-1}. Combining these findings, we can conclude that the activation barrier associated with dehydrogenation of 1-Fe$^+$ amounts to ca. 12 kcal mol^{-1}. Even if we

assume BDE(C$_6$H$_6$–Fe$^+$) = 55 kcal mol^{-1}, as derived by Freiser and coworkers [2b], the activation barrier associated with dehydrogenation of 1-Fe$^+$ would not exceed 20 kcal-mol^{-1}. Furthermore, this figure represents an upper limit for the height of the barrier, since other cooling processes which may eventually lead to stabilization of 1-Fe$^+$ were not considered, e.g. energy uptake by the evaporated ligand.

Although one might argue about the accuracy of the activation barrier obtained by this approach, it is apparent that the energy demand for the Fe$^+$-mediated C–H bond activation and subsequent dehydrogenation of 4-heptanone is surprisingly small. Such low activation barriers are in accord not only with the high regiospecificity in the Fe$^+$-mediated remote functionalization of ketones [13] and the observation of consecutive neutral losses from metastable ketone–Fe$^+$ complexes [6b], but also with the previously reported observation of diastereospecific C–H bond activation [7,16] and the operation of an Ingold–Thorpe effect in the dehydrogenation of ketone–Fe$^+$ complexes [17]. In particular, the subtle steric effects which are involved in the two latter experiments are due to small energy differences not exceeding a few kilocalories per mole; thus, they will only become apparent when the activation barrier associated with dehydrogenation is small, since otherwise these tiny energetic differences would not matter.

As has been demonstrated in previous studies, the energy demand for the dehydrogenation of ketones with alkyl chains larger than propyl is even more facile [6a,16]. Therefore, it is not surprising that the generation and mass selection of unreacted ketone–Fe$^+$ complexes with ketones bearing larger side chains can hardly be achieved under FTICR conditions [19a]. Moreover, it becomes questionable whether these ions are stable towards collisions with the thermalizing buffer gas (e.g. argon). Indeed, all our efforts to mass select thermalized 2-hexanone–Fe$^+$ were always accompanied by significant dehydrogenation to yield the corresponding 5-hexen-2-one–Fe$^+$ complex, which may be traced back to the intrinsic reactivity of the complex and/or the mass selection procedure [16a,19a]. Moreover, even the detection of an ion with such a low threshold towards fragmentation may become difficult under the experimental conditions, since dehydrogenation products may also be formed during ion excitation and detection. For this reason we did not extend our experiments to larger substrates, and we conclude that the energy demands for Fe$^+$-mediated dehydrogenation of ketones bearing even longer alkyl side chains are even lower as compared with that of 4-heptanone. Finally, the finding that in the unimolecular dissociation of metastable 1-Fe(CO)$^+$ dehydrogenation is not observed indicates that the CO ligand raises the activation barrier for bond activation substantially, such that only loss of the ligand, but not that of H$_2$, is observed experimentally.

4. Conclusions

Hitherto, not many experimental studies have addressed the effects of ligation on a particular gas phase ion–molecule reaction in great depth and in a systematic manner. As born out in this study, the additional ligands may cause two quite opposite effects: either the ligand simply acts as a spectator ("innocent" ligand) which moderates the intrinsic reactivity of the bare metal ion in terms of energetics, but does not drastically change the reaction mechanisms and regioselectivities, or the ligand is actively involved in the reaction and promotes and participates in new chemical transformations. In the present study the acetylene and the butadiene ligands belong to the latter category in that they serve as acceptors for the hydrogen atoms being released by Fe^+-mediated C–H bond activation of 4-heptanone. Further studies on the role of the functional group, e.g. ketones vs. nitriles, on the gas phase chemistry of transition metal ions are indicated.

With respect to the use of isotopic labelling, our approach bears a different intention as compared with most of the previous gas phase organometallic studies in that the KIE is not used to examine the reaction mechanism of metal-mediated dehydrogenation itself. Instead, the KIE associated with H_2–HD losses is used to monitor the occurrence of side reactions which would prevent the application of the ligand exchange reaction scheme used here, its energetic considerations in particular. Moreover, the present study demonstrates how data from unimolecular dissociation of metastable ions in a tandem mass spectrometer can be fruitfully combined with results of ion–molecule reactions in a FTICR instrument. Thus, albeit these experimental approaches are indeed quite different, they complement each other quite well [18,19a,22a].

Finally, the fact that remote functionalization of hydrocarbon backbones by metal cations is associated with a small activation barrier and is not completely impeded by additional dative ligands opens up the fascinating perspective to realize regioselective metal-mediated functionalization of remote C–H in the condensed phase and may stimulate further research.

Acknowledgments

Constructive comments by the reviewers are appreciated.

References and notes

[1] See for example: (a) A.E. Shilov, *Activation of Saturated Hydrocarbons by Transition Metal Complexes*, Reidel, Boston, MA, 1984. (b) P.R. Ortiz de Montellano (ed.), *Cytochrome P-450: Structure, Mechanism and Biochemistry*, Plenum, New York, 1986. (c) C.L. Hill (ed.), *Activation and Functionalization of Alkanes*, Wiley, New York, 1989.

[2] For recent reviews, see: (a) S.W. Buckner and B.S. Freiser, *Polyhedron, 7* (1988) 1583. (b) K. Eller and H. Schwarz, *Chem. Rev., 91* (1991) 1121. (c) K. Eller, *Coord. Chem. Rev., 126* (1993) 93.

[3] For representative examples, see: (a) R. Houriet, L.F. Halle and J.L. Beauchamp, *Organometallics, 2* (1983) 1818. (b) M.A. Tolbert and J.L. Beauchamp, *J. Am. Chem. Soc., 106* (1984) 8117. (c) S.D. Hanton, R.J. Noll and J.C. Weisshaar, *J. Phys. Chem., 94* (1990) 5655. (d) R.H. Shultz and P.B. Armentrout, *J. Am. Chem. Soc., 113* (1991) 729. (e) P.A.M. van Koppen, J. Brodbelt-Lustig, M.T. Bowers, D.V. Dearden, J.L. Beauchamp, E.R. Fisher and P.B. Armentrout, *J. Am. Chem. Soc., 113* (1991) 2359. (f) P.A.M. van Koppen, M.T. Bowers, E.R. Fisher and P.B. Armentrout, *J. Am. Chem. Soc., 116* (1994) 3780.

[4] (a) B.D. Radecki and J. Allison, *J. Am. Chem. Soc., 106* (1984) 946. (b) S.J. Babinec and J. Allison, *J. Am. Chem. Soc., 106* (1984) 7718. (c) S. Karraß and H. Schwarz, *Helv. Chim. Acta, 72* (1989) 633. (d) S. Karraß, K. Eller, C. Schulze and H. Schwarz, *Angew. Chem., 101* (1989) 634; *Angew. Chem., Int. Edn. Engl., 28* (1989) 607. (e) S. Karraß, K. Eller and H. Schwarz, *Chem. Ber., 123* (1990) 939. (f) S. Karraß and H. Schwarz, *Organometallics, 9* (1990) 2034. (g) L.-Z. Chen and J.M. Miller, *J. Chem. Soc., Dalton Trans.,* (1993) 1897.

[5] (a) J. Allison and D.P. Ridge, *J. Am. Chem. Soc., 101* (1979) 4998. (b) A. Tsarbopoulos and J. Allison, *J. Am. Chem. Soc., 107* (1985) 5085. (c) T. Prüsse and H. Schwarz, *Organometallics, 8* (1989) 2856. (d) T. Prüsse, J. Allison and H. Schwarz, *Int. J. Mass Spectrom. Ion Processes, 107* (1991) 553.

[6] (a) R.C. Burnier, G.D. Byrd and B.S. Freiser, *J. Am. Chem. Soc., 103* (1981) 4360. (b) D. Schröder and H. Schwarz, *J. Am. Chem. Soc., 112* (1990) 5947.

[7] D. Schröder, W. Zummack and H. Schwarz, *J. Am. Chem. Soc., 116* (1994) 5857.

[8] (a) C.B. Lebrilla, C. Schulze and H. Schwarz, *J. Am. Chem. Soc., 109* (1987) 98. (b) C.B. Lebrilla, T. Drewello and H. Schwarz, *J. Am. Chem. Soc., 109* (1987) 5639. (c) R.M. Stepnowski and J. Allison, *Organometallics, 7* (1988) 2097. (d) T. Prüsse, C.B. Lebrilla, T. Drewello and H. Schwarz, *J. Am. Chem. Soc., 110* (1988) 5986. (e) G. Czekay, T. Drewello, K. Eller, W. Zummack and H. Schwarz, *Organometallics, 8* (1989) 2439. (f) K. Eller, W. Zummack, H. Schwarz, L.M. Roth and B.S. Freiser, *J. Am. Chem. Soc., 113* (1991) 833. (g) K. Eller, S. Karrass and H. Schwarz, *Organometallics, 11* (1992) 1637. (h) G. Hornung, D. Schröder, H. Schwarz, *J. Am. Chem. Soc., 117* (1995) 8192.

[9] D.J. Hankinson, C.B. Miller and J. Allison, *J. Phys. Chem., 93* (1989) 3624.

[10] For an example of nearly complete H–D equilibration in a relatively large hydrocarbon backbone, see: J. Schwarz and H. Schwarz, *Chem. Ber., 126* (1993) 1257.

[11] (a) R. Breslow, *Chem. Soc. Rev., 1* (1972) 553. (b) R. Breslow, *Acc. Chem. Res., 13* (1980) 170. (c) R. Breslow, A. Adams, T. Guo and J. Hunger, *Lect. Heterocycl. Chem., 9* (1987) 43.

[12] (a) H. Schwarz, *Acc. Chem. Res.*, 22 (1989) 283. (b) G. Czekay, T. Drewello, K. Eller, C.B. Lebrilla, T. Prüsse, C. Schulze, N. Steinrück, D. Sülzle, T. Weiske and H. Schwarz, in H. Werner and G. Erker (eds.), *Organometallics in Organic Synthesis 2*, Springer, Heidelberg, 1989, p. 203.

[13] (a) G. Czekay, K. Eller, D. Schröder and H. Schwarz, *Angew. Chem.*, 101 (1989) 1306; *Angew. Chem., Int. Edn. Engl.*, 28 (1989) 1277. (b) D. Schröder and H. Schwarz, *Chimia*, 43 (1989) 317. (c) D. Schröder, F. Jeske and H. Schwarz, *Int. J. Mass Spectrom. Ion Processes*, 107 (1991) 559.

[14] R.H. Schultz and P.B. Armentrout, *J. Phys. Chem.*, 96 (1992) 1662, and references cited therein.

[15] D. Schröder, *Diploma Thesis*, Technische Universität Berlin, 1989.

[16] (a) D. Schröder, *Ph.D. Thesis*, Technische Universität Berlin, D83, 1993. (b) D. Schröder and H. Schwarz, *J. Am. Chem. Soc.*, 115 (1993) 8818.

[17] D. Schröder, J.H. Bowie, M.B. Stringer and H. Schwarz, *Chem. Ber.*, 124 (1991) 1679.

[18] (a) C.A. Schalley, D. Schröder and H. Schwarz, *J. Am. Chem. Soc.*, 116 (1994) 11089. (b) C.A. Schalley, D. Schröder and H. Schwarz, *Organometallics*, 14 (1995) 317.

[19] (a) D. Schröder, K. Eller, T. Prüsse and H. Schwarz, *Organometallics*, 10 (1991) 2052. (b) Also see: D. Stöckigt, S. Sen and H. Schwarz, *Chem. Ber.*, 126 (1993) 2553. (c) D. Stöckigt and H. Schwarz, *Liebigs Ann.*, (1995) 429.

[20] (a) M.T. Bowers (ed.), *Gas Phase Ion Chemistry*, Academic Press, New York, 1979. (b) J.H. Futrell (ed.), *Gaseous Ion Chemistry and Mass Spectrometry*, Wiley, New York, 1986.

[21] For examples of related approaches to examine energetics of ion–molecule reactions, see: (a) D. Thölmann, D. Flottmann and H.-F. Grützmacher, *Chem. Ber.*, 124 (1991) 2349. (b) B.D. Wladkowski, J.L. Wilbur and J.I. Brauman, *J. Am. Chem. Soc.*, 114 (1992) 9706.

[22] (a) K. Eller and H. Schwarz, *Int. J. Mass Spectrom. Ion Processes*, 93 (1989) 243. (b) K. Eller, W. Zummack and H. Schwarz, *J. Am. Chem. Soc.*, 112 (1990) 621.

[23] (a) B.S. Freiser, *Talanta*, 32 (1985) 697. (b) B.S. Freiser, *Anal. Chim. Acta*, 178 (1985) 137.

[24] R.A. Forbes, F.H. Laukien and J. Wronka, *Int. J. Mass Spectrom. Ion Processes*, 83 (1988) 23.

[25] For further details on ion thermalization, see: (a) D. Schröder, A. Fiedler, M.F. Ryan and H. Schwarz, *J. Phys. Chem.*, 98 (1994) 68. (b) D.E. Clemmer, Y.-M. Chen, F.A. Khan and P.B. Armentrout, *J. Phys. Chem.*, 98 (1994) 6522.

[26] M.S. Foster and J.L. Beauchamp, *J. Am. Chem. Soc.*, 97 (1975) 4808.

[27] (a) G.D. Byrd, R.C. Burnier and B.S. Freiser, *J. Am. Chem. Soc.*, 104 (1982) 3565. (b) B.S. Larsen and D.P. Ridge, *J. Am. Chem. Soc.*, 106 (1984) 1912.

[28] (a) D.L. Rempel, S.K. Huang and M.L. Gross, *Int. J. Mass Spectrom. Ion Processes*, 70 (1986) 163. (b) M. Moini and J.R. Eyler, *Int. J. Mass Spectrom. Ion Processes*, 87 (1989) 29. (c) L. de Koning, *Ph.D. Thesis*, Universiteit van Amsterdam, Amsterdam, 1989.

[29] (a) R. Srinivas, D. Sülzle, T. Weiske and H. Schwarz, *Int. J. Mass Spectrom. Ion Processes*, 107 (1991) 368. (b) R. Srinivas, D. Sülzle, W. Koch, C.H. DePuy and H. Schwarz, *J. Am. Chem. Soc.*, 113 (1991) 5970.

[30] (a) S.G. Lias, J.E. Bartmess, J.F. Liebman, J.L. Holmes, R.D. Levin and W.G. Mallard, *J. Phys. Chem. Ref. Data*, 17 (Suppl. 1) (1988). (b) J.E. Bartmess, *NIST Negative Ion Energetics Database*, Version 3.01, Standard Reference Database 19B, National Institute of Standards and Technology, October 1993. (c) J. Berkowitz, G.B. Ellison and D. Gutman, *J. Phys. Chem.*,

98 (1994) 2744. (d) For an excellent survey of accurate BDEs of small organometallic ions, see: P.B. Armentrout and B.L. Kickel, in B.S. Freiser (ed.), *Organometallic Ion Chemistry*, submitted for publication.

[31] D. Schröder, J. Hrušák, R.H. Hertwig, W. Koch, P. Schwerdtfeger and H. Schwarz, *Organometallics*, 14 (1995) 312.

[32] (a) For this concept, see: S.A. McLuckey, A.E. Schoen and R.G. Cooks, *J. Am. Chem. Soc.*, 104 (1982) 848. (b) For an application to metal-ligand complexes, see: L.Z. Chen and J.M. Miller, *Org. Mass Spectrom.*, 27 (1992) 883. (c) For a general discussion, see: J.S. Brodbelt-Lustig and R.G. Cooks, *Talanta*, 36 (1989) 225. (d) For a review, see: R.G. Cooks, J.S. Pattrick, T. Kotiaho and S.A. McLuckey, *Mass Spectrometry Rev.*, to be published.

[33] Because of the experimental uncertainties, entropic effects in terms of $\Delta\Delta S$ have been completely neglected. However, the neglect of entropy effects is not a matter of serious concern in the system of interest; also see Ref. [32].

[34] B.A. Rumpf, C.E. Allison and P.J. Derrick, *Org. Mass Spectrom.*, 21 (1986) 295.

[35] (a) R.C. Dunbar, G.T. Uechi and B. Asamoto, *J. Am. Chem. Soc.*, 116 (1994) 2466. (b) D. Stöckigt, J. Hrušák and H. Schwarz, *Int. J. Mass Spectrom. Ion Processes*, to be published. (c) For a review, see: R.C. Dunbar, *Mass Spectrom. Rev.*, 11 (1992) 309.

[36] (a) D.B. Jacobson and B.S. Freiser, *J. Am. Chem. Soc.*, 105 (1983) 7484. (b) A. Tsarbopoulos and J. Allison, *Organometallics*, 3 (1984) 86. (c) J. Allison, A. Mavridis and J.F. Harrison, *Polyhedron*, 7 (1988) 1559. (d) R. Stepnowski and J. Allison, *J. Am. Chem. Soc.*, 111 (1989) 449. (e) R.L. Hettich and B.S. Freiser, *Organometallics*, 8 (1989) 2447. (f) H. Becker, D. Schröder, W. Zummack and H. Schwarz, *J. Am. Chem. Soc.*, 116 (1994) 1096.

[37] J.A. Martinho Simões and J.L. Beauchamp, *Chem. Rev.*, 90 (1990) 629.

[38] T.J. MacMahon, T.C. Jackson and B.S. Freiser, *J. Am. Chem. Soc.*, 111 (1989) 421.

[39] B.S. Freiser, personal communication.

[40] C.W. Bauschlicher, Jr., H. Partridge and S.R. Langhoff, *J. Phys. Chem.*, 96 (1992) 3273.

[41] C. Lifshitz, *Mass Spectrom. Rev.*, 12 (1993) 261.

[42] F. Meyer, F.A. Khan and P.B. Armentrout, *J. Phys. Chem.*, submitted for publication.

[43] S. Karraß, D. Schröder and H. Schwarz, *Chem. Ber.*, 125 (1992) 751.

[44] (a) L.M. Jackman, *Adv. Org. Chem.*, 2 (1960) 329. (b) G. Brieger and T.J. Nestrick, *Chem. Rev.*, 74 (1974) 567. (c) Also see: T. Gerres and A. Heesing, *Chem. Ber.*, 125 (1992) 1431, 1439, and references cited therein.

[45] A small amount of C–D bond activation of the α-position in 1b/Fe(C_4H_6)$^+$ leads also to unimolecular HD losses (H_2:HD = 100:2); mostly likely this is due to partial H/D equilibration of the complex (also see Ref. [39]).

[46] (a) D. Schröder, D. Sülzle, J. Hrušák, D.K. Böhme and H. Schwarz, *Int. J. Mass Spectrom. Ion Processes*, 110 (1991) 145. (b) R. Bakhtiar, J.J. Drader and D.B. Jacobson, *J. Am. Chem. Soc.*, 114 (1992) 8304.

[47] For example, see: (a) P.J. Marinelli and R.R. Squires, *J. Am. Chem. Soc.*, 111 (1989) 4101. (b) T.F. Magnera, D.E. David, D. Stulik, R.G. Orth, H.T. Jonkin and J. Michl, *J. Am. Chem. Soc.*, 111 (1989) 5036. (c) M. Rosi and C.W. Bauschlicher, Jr., *J. Chem. Phys.*, 92 (1990) 1876. (d) P.R. Kemper, J. Bushnell, P.v. Koppen and M.T. Bowers, *J. Phys. Chem.* 97 (1993) 1810. (e) F.A. Khan, D.E. Clemmer, R.H. Schultz and P.B. Armentrout, *J. Phys. Chem.*, 97 (1993) 7978.